Elucidation of the Nature of Structural Heterogeneity During Alkali Leaching of Non-activated and Mechanically Activated Boehmite (γ-AlOOH)

RAKESH KUMAR and THOMAS C. ALEX

Crystal joints and faces in non-activated boehmite and, state of agglomeration of particles, degree of amorphization, microcrystallite dimension and, strain in mechanically activated boehmite are indicators of structural heterogeneity which influences reactivity of the solid phase. The focus of this paper is on understanding the manifestation of the heterogeneity during alkali leaching of a boehmite (specific surface area—263 m^2/g), without and with mechanical activation using planetary milling up to 240 minutes. A two-prong strategy is used for this purpose which involved analysis of the kinetics of leaching by a model-free approach using 'isoconversional method' and, in parallel, characterization of the reacting solid after different durations of leaching. Unlike model-fitting methods, the kinetic analysis revealed sample-dependent variation of apparent activation energy with fraction leached. Changes observed in the morphology of samples (by SEM), particle size distribution (by laser diffraction), and crystalline nature (by powder X-ray diffraction) are used to explain activation energy changes and propose mechanisms of leaching. The effect of mechanical activation on rate constant is assessed and it has been found that up to ~23-fold increase in rate is possible depending on the activation time, leaching temperature, and fraction leached. Further, based on binary correlations between activation energy at different fractions leached and initial characteristics of the samples, it is found that the leaching is predominantly influenced by structural changes during milling, namely, degree of amorphization, microcrystallite dimension, and strain, *vis-à-vis* specific surface area. Significantly, the paper highlights limitation of model-fitting methods used by most researchers to analyze the kinetics of leaching, especially for mechanically activated minerals.

I. INTRODUCTION

BOEHMITE is an aluminum oxyhydroxide (γ-AlOOH) (orthorhombic; $a = 0.36936$ nm, $b = 1.2214$ nm, $c = 0.28679$ nm; space group *Cmcm*) consisting of double layer of $AlO_4(OH)_2$ octahedra which are linked by H-bond between hydroxyl groups.[1,2] Alkali leaching of boehmite is of interest in the Bayer process of alumina production[3] and processing of nuclear wastes.[4] Several investigations have focused on alkali leaching of boehmite.[2–19] The kinetics of alkali leaching is described in terms of 'shrinking core model with surface reaction'[4,13,19] and 'first-order chemical reaction.'[15–17] Most studies have focused on the effect of alkali concentration and temperature on boehmite solubility.[6–14] Widely different solubility of boehmite is reported in literature. Grénman *et al.*[14] observed only 4 pct dissolution after 3 hours of leaching in 6 M NaOH solution at 358 K (85 °C). High solubility of boehmite (up to 60 pct) has been reported for nano-size (0.07 to 0.1 μm) boehmite by Packter[9] and high surface area

(264 m^2/g) boehmite by Alex *et al.*[18,19] under ambient pressure leaching. In spite of different reported solubilities, the effect of nature of solid phase, *e.g.*, purity (chemical and structural), specific surface area, porosity, crystallite size, *etc.*,[20,21] have not been adequately addressed.

Mechanical activation, the term introduced by Smékal[23, p. 7572] to describe change in reaction ability of solids due to physico-chemical changes during milling, is used to enhance the leachability of Al-oxyhydroxide minerals, including boehmite.[2,18,22–31] After 120 minutes of mechanical activation in a planetary mill, an increase in leachability from 58 to 88 pct and 12 to 92 pct is observed during alkali leaching (temperature—363 K (90 °C), alkali concentration—180 g/l Na_2O, leaching time—30 minutes) for boehmite prepared by thermal and hydrothermal transformation of gibbsite, respectively.[18,30] Kinetics of alkali leaching of mechanically activated boehmite has been explained in terms of 'second-order reaction model.'[31]

The nature of solid phase may change continuously during leaching. For example, higher solubility of edge, corner, and grain boundary regions *vis-à-vis* crystal faces is observed during initial stage of leaching of phase pure boehmite.[19] Structural heterogeneity is an essential feature of mechanically activated solids.[32–35] The nature of solid changes continuously during chemical

RAKESH KUMAR, Chief Scientist and Head of Division, and THOMAS C. ALEX, Principal Scientist, are with the Metal Extraction and Forming Division, National Metallurgical Laboratory, Jamshedpur 831 007, India. Contact e-mail: rakesh.nmlindia@gmail.com

reactions as high energy regions (*i.e.*, regions of solid phase characterized by greater structural disorder) are preferentially attacked.[34,35] Alex *et al.*[19,31] have used model-fitting methods to analyze the kinetics of boehmite leaching. The model-fitting methods are inadequate to provide a complete and realistic picture. We observed that the quality of fit during model-fitting is generally far from good and, the models are fitted only to a partial range of fraction leached and not the entire range.[19,31] Further, there is disconnect between the model-fitting analysis and characterization of the leach residues, *i.e.*, the changing nature of solid is not explained by the model since it assumes structurally uniform solid. Consequently, nature of structural heterogeneity present in the samples and its significance are not well understood. In order to address the inadequacy of model-fitting methods, model-free analysis approach involving isoconversional method[36–38] is employed in this study to investigate the kinetics of alkali leaching of boehmite, without and with mechanical activation. Isoconversional method permits the estimation of activation energy as a function of fraction of boehmite leached. In parallel efforts, the leach residues obtained after different duration of leaching are characterized in terms of morphology, particle size distribution, and crystallinity. The results of isoconversional method and characterization of leach residues are collectively presented to elucidate the manifestation of structural heterogeneity with the progress of leaching. Implications of the findings are highlighted in the context of reactivity of mechanically activated solids.

II. MATERIALS AND METHODS

A. *Boehmite Sample*

Phase pure boehmite [JCPDS No. 83-2384] used in the study was synthesized by thermal transformation of Bayer's process gibbsite as described in an earlier publication.[18] The median particle size (d_{50}) of the sample was 110 μm. The geometrical specific surface area (SSA_{Geo}) and BET specific surface area (SSA_{BET}) of the sample were 0.10 and 263 m^2/g, respectively, indicating highly porous nature of the sample.

B. *Mechanical Activation*

Mechanical activation of the sample was carried out using a batch type planetary mill (Pulverisette P6, Fritsch GmbH, Germany) under the following conditions: sample weight—30 g, media—steel balls of diameter 10 mm, ball to powder ratio—30:1, rotational speed—400 min^{-1}. The samples were mechanically activated for different durations (t_{MA} = 5, 15, 30, 60, 120, and 240 minutes). Milling was stopped intermittently to prevent overheating.[18]

C. *Leaching*

Leaching was carried out in a thermostatically controlled continuously stirred cylindrical glass vessel.

Sodium hydroxide solution (180 g/l Na$_2$O) was used for leaching. In all experiments, the initial solid: liquid ratio and stirring speed were fixed at 1:8 (mass, g: volume, ml) and 400 min^{-1}, respectively. The boehmite sample was transferred to the reactor after the temperature of the leaching medium stabilized at the set value [±1 K (1 °C)]. The duration of leaching was varied up to 60 minutes. At the end of leaching experiment, undissolved boehmite was separated immediately by centrifuging. The separated residue was washed with hot water several times, dried at 378 K (105 °C) for 2 hours, cooled in a desiccator and weighed. The extent of dissolution of boehmite was calculated from the weight of the residue. The experimental reproducibility was in the error limits ±2 to 3 pct (based on the average of three experiments for randomly selected points). To cross check the results obtained from residue analysis, leach solutions were also analyzed randomly for dissolved alumina using standard EDTA method;[39] the match between the results obtained using solid and solution analysis was within ±5 pct. The leaching results have been expressed in terms of fraction dissolved (α) or weight of the sample dissolved per liter of leach liquor.

D. *Characterization of Mechanically Activated Boehmite and Leach Residues*

Mechanically activated samples were characterized in terms of morphology, particle size distribution, surface area, and structural changes. Morphological features were examined under scanning electron microscope (SEM) (Model: S-3400N, Hitachi, Japan). Particle size distribution and geometrical specific surface area (SSA_{Geo}) were determined using a laser diffraction particle size analyzer (Model: Mastersizer, Malvern, UK). BET specific surface area (SSA_{BET}) was estimated by N$_2$ adsorption method using a surface area analyser (Model: ASAP2020, Micromeritics, Instrument Corporation). Powder X-ray diffraction (XRD) patterns, in the 2θ range of 10 to 80°, were recorded at a scanning rate of 1°/min using a diffractometer (Model: Discover D8, Bruker AXS GmbH, Germany) with CuK$_\alpha$ radiation. The patterns were analyzed for the characterization of the samples in terms of degree of amorphization (A_m), microcrystalline dimension (MCD), and microstrain (ε). A_m was calculated from the ratio of standardized integrated intensities of (020) XRD peak of mechanically activated and non-activated boehmite[30,40] and MCD and microstrain (ε) were estimated from full width half maxima analysis.[18] Some of the activated samples were also examined under transmission electron microscope (TEM) (Model: CM200, Philips, Netherlands). Carbon-coated grids were used for sample preparation. Bright field micrographs and corresponding selected area electron diffraction patterns were recorded using TEM at 200 kV. The washed and dried leach residues obtained after different leaching intervals were also characterized in terms of morphology, particle size distribution, and crystallinity using similar techniques as employed for the mechanically activated samples.

III. RESULTS AND DISCUSSION

A. Nature of Non-activated and Mechanically Activated Boehmite

Figure 1 shows typical morphological features of the non-activated and mechanically activated boehmite. The non-activated boehmite retains the morphology of the gibbsite which was used for its synthesis. The morphology comprises of agglomerate of platelets (Figure 1(a)). In addition, slit type pores formed during thermal transformation of gibbsite to boehmite are present in the sample (Figure 1(b)). The boehmite particle breaks during milling and simultaneously fuse together to form agglomerated particles. The extent of agglomeration depends on the milling time as shown typically for 3 minutes and 60 minutes milled samples in Figures 1(c) and (d), respectively.

The physico-chemical characteristics of the samples, viz., characteristic particle diameters (d_{10}, d_{50}, d_{90}); geometrical specific surface area (SSA_{Geo}) and BET specific surface area (SSA_{BET}); and degree of amorphization (A_m), MCD, and microstrain (ε) are summarized in Table I.

A decrease followed by an increase in characteristic particle diameters (Table I) is the result of simultaneous breakage and agglomeration of particles by fusing as indicated by morphological characterization by SEM (Figures 1(c) and (d)). A large difference in geometrical and BET specific surface area, SSA_{Geo} and SSA_{BET}, is attributed to the highly porous nature of the samples. The BET specific surface area shows an anomalous decrease from 263.1 to 67.6 m^2/g after 240 minutes of milling. A similar anomalous decrease has been reported by Kitamura and Senna[40] for the boehmite which was also synthesized by thermal transformation of gibbsite. The evolution of surface area during the milling of boehmite may result from a number of phenomena, namely, breakage and fusing together of particles, change in existing pore structure, and possible creation of new pores due to the escape of water resulting from milling-induced dehydroxylation.[18,23,30] It appears that the effect of coalescence of small pores during milling dominates and is responsible for the anomalous decrease in SSA_{BET}.[18] During pore size analysis of the samples, it is found that the average pore diameter increases from 3.2 to 12.8 nm as the milling time increases from 0 to 240 minutes. Assuming spherical pores, based on the pore diameters, ~16-fold decrease in surface area is expected. However, the observed decrease in SSA_{BET} is much less (~4-fold); this signifies the complexity of the mechanisms involved in the evolution of surface area and possible contribution from newly formed pores due to milling-induced dehydroxylation.[23] It is interesting to note that the anomalous decrease in SSA_{BET} is unique to the very high surface area (263.1 m^2/g) boehmite prepared by thermal transformation of gibbsite.[18,40] In
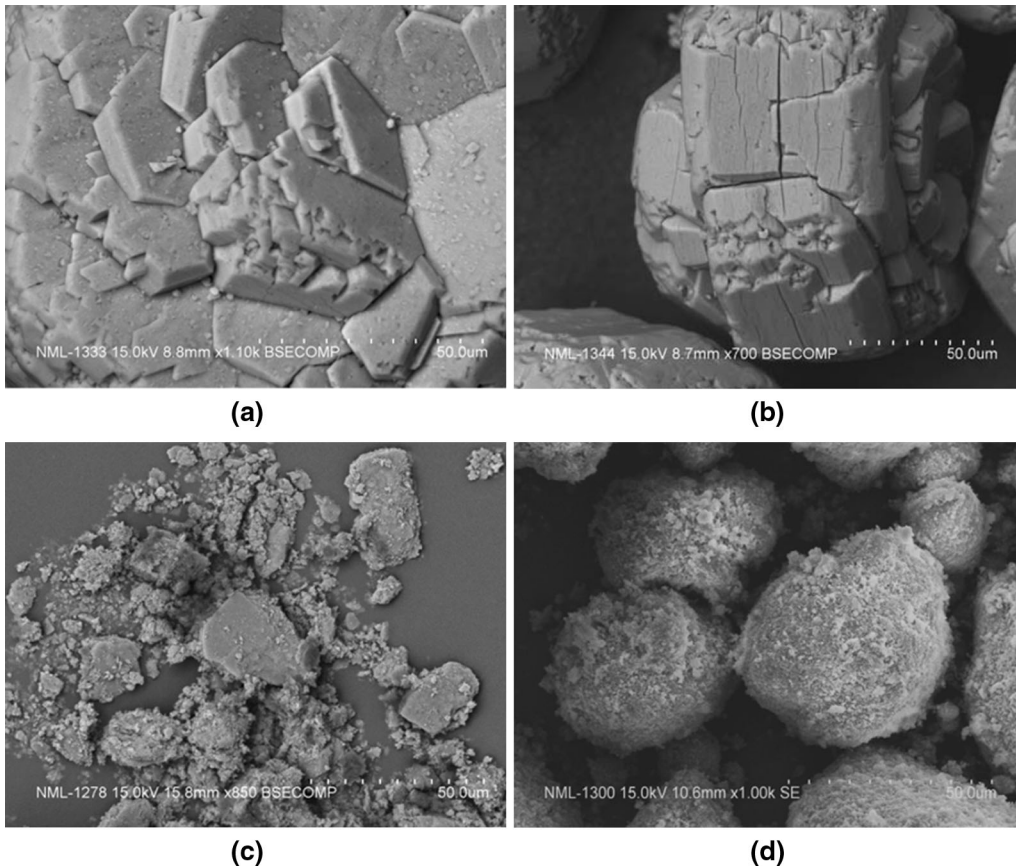

Fig. 1—SEM micrographs showing typical morphological features: (a), (b) boehmite without activation; (c) and (d) after 3 and 60 min of milling, respectively.

Table I. Physico-chemical Characteristics of the Non-activated and Mechanically Activated Boehmite Samples (Compiled from Alex et al.,[18] Except Degree of Amorphization Data)

Milling Time (t_{MA}) (min)	Characteristic Diameters (μm)			Specific Surface Area (SSA) (m²/g)		Degree of Amorphization (A_m), Microcrystalline Dimension (MCD), and Microstrain (ε)		
	d_{10}	d_{50}	d_{90}	SSA_{Geo}	SSA_{BET}	A_m (pct)	MCD (nm)	ε
0	77	110	153	0.10	263.1	0	252.8	0.0023
15	0.32	1.8	29.8	2.71	201.2	31.4	212.2	0.0030
30	0.32	2.4	35.9	2.59	188.9	41.7	152.8	0.0036
60	0.33	3.6	39.2	2.42	143.1	61.4	68.6	0.0038
90	0.34	4.8	43.0	2.25	122.6	63.8	54.6	0.0041
120	0.35	5.8	43.7	2.15	115.1	71.2	34.5	0.0043
240	0.36	5.0	42.2	2.14	67.6	85.8	17.2	0.0047

the case of lower surface area boehmite prepared by hydrothermal transformation of gibbsite, the usual increase in specific surface area (from 2.98 to ~34 m²/g after 240 minutes milling) is observed and it is attributed to the formation of new pore structure due to milling-induced dehydroxylation.[23,30]

The degree of amorphization (A_m) and MCD and microstrain (ε) values undergo changes with milling time (Table I). The degree of amorphization increases to ~86 pct after 240 minutes of milling. During the same period, the microcrystallite dimension decreases from 253 to 17 nm and microstrain increases from 0.0023 to 0.0047. The amorphization of boehmite during milling is associated with simultaneous dehydroxylation.[22,23] A decrease in crystallite size and an increase in amorphization with milling time is supported by transmission electron micrographs (Figures 2(a), (c), and (e)) and corresponding selected area electron diffraction patterns (Figures 2(b), (d), and (f)). Large crystals (>200 nm) in the unmilled boehmite give single-crystal spot diffraction pattern (Figures 2(a), (b)). The crystals become increasingly finer in 60 and 240 minutes milled samples (Figures 2(c), (e)) and diffraction pattern changes to that of a typical polycrystalline material (Figures 2(d)) and close to amorphous material ((Figure 2(f)). The values of A_m, MCD, and ε are mean values and in real samples correspond to a distribution. The values can be treated as discrete for macrokinetic studies.[32,33]

B. α-t Plots for Boehmite Leaching

Boehmite dissolves in alkali as sodium aluminate according to the following reaction:[3–5,12–17,41]

$$\gamma - AlOOH_{(s)} + NaOH_{(aq)} \rightarrow Na^+ Al(OH)_4^{-1}{}_{(aq)} \quad [1]$$
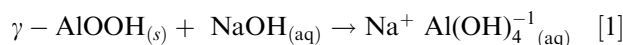
Figures 3(a) through (c) show the fraction of boehmite leached (α) as a function of time (t) at different temperatures, 343 K, 353 K, and 363 K (70 °C, 80 °C, and 90 °C), for the boehmite samples mechanically activated for different durations (t_{MA}) up to 240 minutes. For comparison, the results for the non-activated boehmite (t_{MA} = 0) are also included in the Figure 3. The beneficial effect of mechanical activation is evident from the results presented. After 60 minutes of leaching,

with an increase in milling time from 0 to 240 minutes, the value of α increases from 0.33 to 0.81, 0.53 to 0.89, and 0.64 to 0.93 at 343 K, 353 K, and 363 K (70 °C, 80 °C, and 90 °C), respectively. Based on these results, it can be inferred that dissolution from mechanically activated boehmite samples is less sensitive to rise in temperature as compared to the non-activated boehmite sample.

The maximum attainable value of α (= 1) corresponds to boehmite solubility of 85 g/l Al₂O₃ and alkali to caustic weight ratio (a/c ratio) of 0.47. Boehmite is metastable in the temperature regime in which leaching experiments are carried out.[42,43] Therefore, the equilibrium solubility is governed by the solubility of gibbsite which is the stable phase.[18] The equilibrium solubility of alumina in caustic solution (180 g/l) at 343 K and 363 K (70 °C and 90 °C) is estimated using published literature.[43–45] The equilibrium solubility is found to be ~120 g/l (a/c = 0.65) and 147 to 166 g/l Al₂O₃ (a/c = 0.82 to 0.91) at 343 K and 363 K (70 °C and 90 °C), respectively. Thus, in all cases, the observed solubility was much less than equilibrium solubility and rules out back reaction leading to precipitation.

C. Kinetics Analysis and the Estimation of Activation Energy

Model-free analysis based on isoconversional method is used to study the kinetics of alkali leaching of boehmite. The method adopted calculates the reaction activation energy (E_a) without any model assumption. The basis of isoconversional method can be derived using the isothermal rate law which can be written as[38]

$$g(\alpha) = Z \exp\left(-\frac{E_a}{RT}\right)t, \quad [2]$$

(where $g(\alpha)$ = functional form of integral reaction model, Z = pre-exponential factor, R = gas constant, T is temperature in degree K, t is reaction time)

By taking the logarithm, Eq. [2] can be expressed as

$$\ln g(\alpha) = \ln Z - \frac{E_a}{RT} + \ln t. \quad [3]$$
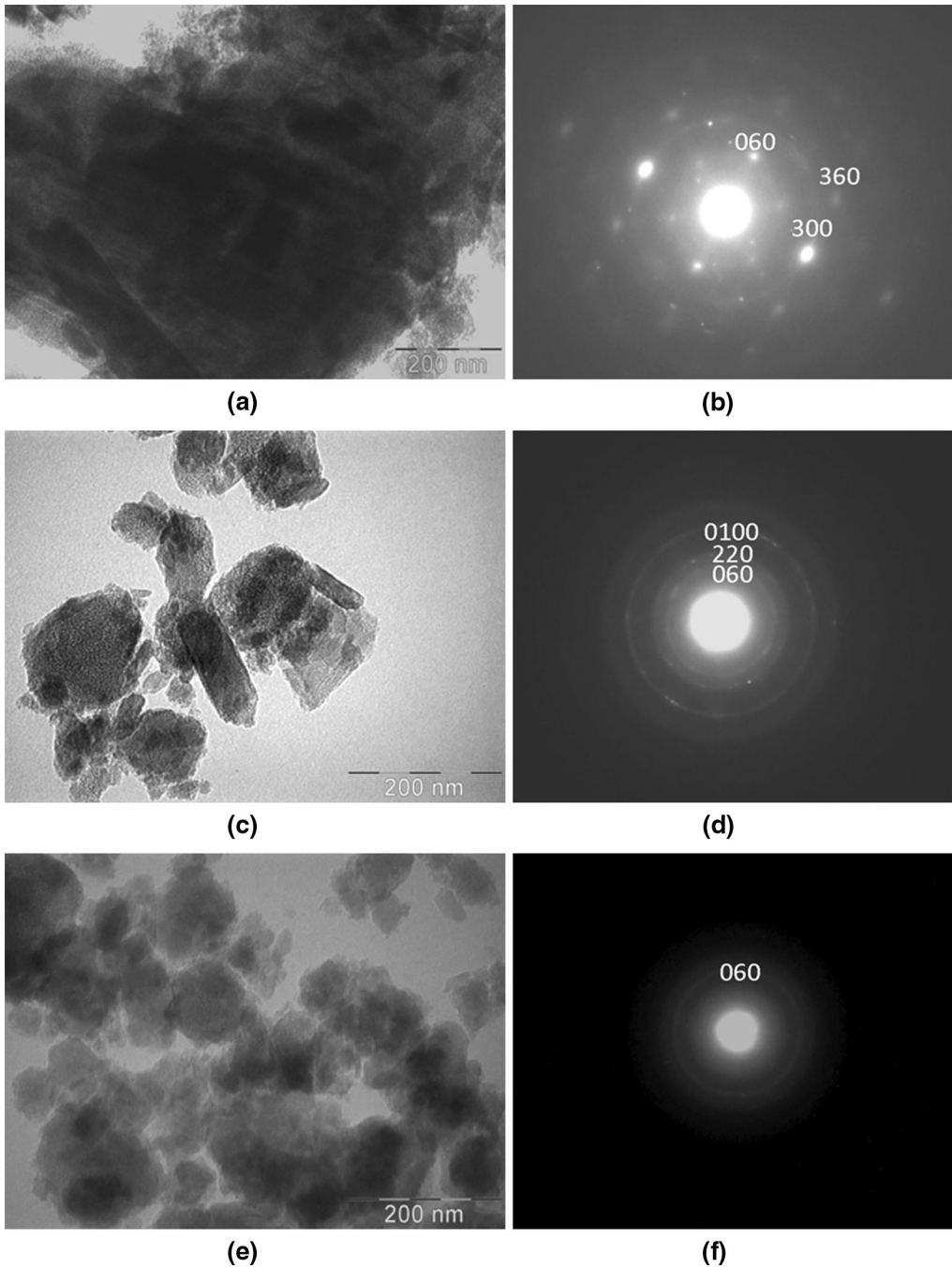
Equation [3] can be further rearranged to give

Fig. 2—TEM micrographs and corresponding selected area electron diffraction patterns for boehmite after different durations of milling: (*a*), (*b*) 15 min, (*c*), (*d*) 60 min, and (*e*), (*f*) 240 min.

$$-\ln t = \ln\left(\frac{Z}{g(\alpha)}\right) - \frac{E_a}{RT}. \qquad [4]$$

A plot of $-\ln t$ *vs* $1/T$ for each α gives E_a from the slope for that α, regardless of the model, according to the following equation:

$$-\ln t_\alpha = \ln\left(\frac{Z}{g(\alpha)}\right)_\alpha - \frac{E_{a\alpha}}{RT}. \qquad [5]$$

Based on Eq. [5], the isoconversional method allows evaluation of activation energy ($E_{a\alpha}$) at progressively increasing values of fraction reacted (α). For each reacting solid, calculations from several α-t curves at different temperatures are performed on the same value of conversion (α), thus the name isoconversional.[38] The intercept in Eq. [5] gives value of $\ln[Z/g(\alpha)]_\alpha$ and estimation of pre-exponential factor (Z) requires modelistic assumption. Therefore, the method only reports
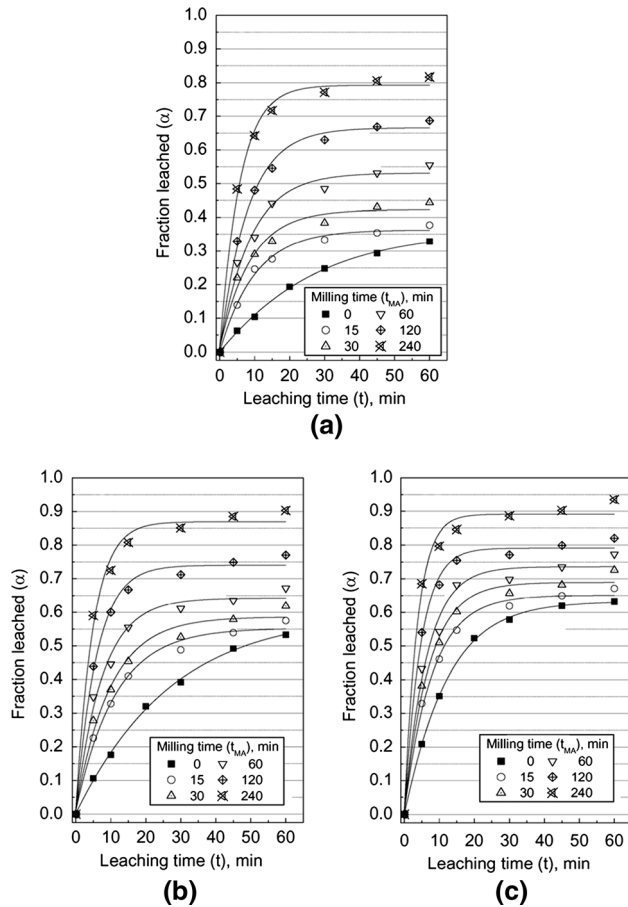
Fig. 3—Fraction leached (α) *vs* time (t) plots at different temperatures for boehmite samples milled for different duration of time : (*a*) 343 K (70 °C); (*b*) 353 K (80 °C); and (*c*) 363 K (90 °C) [Na$_2$O concentration—180 g/l, stirring speed—400 min^{-1}] (leaching data taken from[31]).

the value of $E_{a\alpha}$ and pre-exponential factor values are not reported.[38]

The α-t plots in Figures 3(a) through (c) are used to estimate the value of t_α at different temperatures for the non-activated sample (t_{MA} = 0 minutes), as well as the samples which were mechanically activated for different duration (*i.e.*, t_{MA} = 15, 30, 60, 120, and 240 minutes). In order to get the t_α value from experimental α *vs* t data, the data were fitted with a Boltzmann function with a goodness of fit (R^2) value of greater than 0.99. For each sample, t_α values at different temperatures were obtained at an α interval of 0.05 and $\ln t_\alpha$ *vs* $1/T$ plots, as shown in Figure 4, were prepared. The $\ln t_\alpha$ *vs* $1/T$ plots in Figure 4 were linear fit ($R^2 \geq 0.99$). The variation of apparent activation energy ($E_{a\alpha}$), obtained from the slope of linear fit, with fraction leached (α) is given in Figure 5 for the non-activated and mechanically activated boehmite samples. The non-activated boehmite sample shows a higher value of $E_{a\alpha}$ as compared to the mechanically activated samples. $E_{a\alpha}$ decreases with increasing t_{MA}. The value of $E_{a\alpha}$ shows a sample-dependent variation with α. The variation is pronounced for the non-activated sample and, for the mechanically activated sample it diminishes with an increase in the

activation time. Nearly constant value of $E_{a\alpha}$ in the range of α from 0.1 to 0.2 (region marked A in Figure 5, $E_{a\alpha} \sim$ 75 kJ/mol) and 0.4 to 0.5 (region marked B in Figure 5, $E_{a\alpha} \sim$ 98 kJ/mol) is observed for the non-activated sample. The variation $E_{a\alpha}$ with α is steeper for 15 minutes milled sample and $E_{a\alpha}$ gradually become less sensitive to the variation in α as the mechanical activation time increases up to 240 minutes. The range of α (up to ~0.45) over which a nearly constant value of $E_{a\alpha}$ (29.5 ± 0.5 kJ/mol) is observed is highest in the 240 minutes milled sample. The observed variation of $E_{a\alpha}$ with α as obtained by 'isoconversional method' is in sharp contrast with model-fitting methods employed in earlier studies[19,31] where a single value of the activation energy is obtained for each of the samples. While the variations of $E_{a\alpha}$ with α may appear to be in conflict with basic chemical kinetic principles, in reality, it may not be so. Many explanations have been suggested for the variation $E_{a\alpha}$ with α.[38] In the leaching reactions, a variation in activation energy could be observed due to heterogeneous imperfection distribution, *i.e.*, a sample may have structural heterogeneities having different leachability and different samples of the same material (boehmite) may have different imperfection distributions, *i.e.*, no two solid samples are identical, although they may be similar.[18,19,31,34–38] The solid leach residue samples were characterized after different durations of leaching time to elucidate this point.

D. Characterization of Leach Residues

1. Morphological characterization

Figures 6 and 7 show typical SEM micrographs of the leach residues. The SEM micrographs in Figures 6(a) through (d) are for the leach residues obtained for non-activated boehmite sample after 5, 10, 30, and 45 minutes of leaching, respectively, which corresponds to 0.1, 0.18, 0.4, and 0.49 of fraction leached at 353 K (80 °C). During the initial stage of leaching, particle joints become increasingly prominent indicating that these regions are preferentially attacked (Figures 6(a), (b)). As the leaching progresses further (Figure 6(c)), the particles undergo breakage along joints and also show signs of preferential leaching of pore regions. After prolonged duration, leaching is dominated by crystal faces (Figure 6(d)). These results highlight heterogeneous nature of leaching for the non-activated boehmite sample.

The results in Figure 7 are for the leach residues obtained for the mechanically activated samples. Figures 7(a) through (f) show results for 60 and 240 minutes milled samples, respectively. The micrographs presented are for the leach residues obtained after 5, 10, and 30 minutes of leaching which corresponds to fraction-leached values of 0.3, 0.47, and 0.64 and 0.57, 0.85, and 0.87 for the 60 and 240 minutes milled samples, respectively. The agglomerate character of the original activated samples is retained in the leach residues. The agglomerate structure present in 60 minutes milled sample is more heterogeneous in nature *vis-à-vis* 240 minutes sample. In the 60 minutes milled sample, cemented regions which appear to persist down
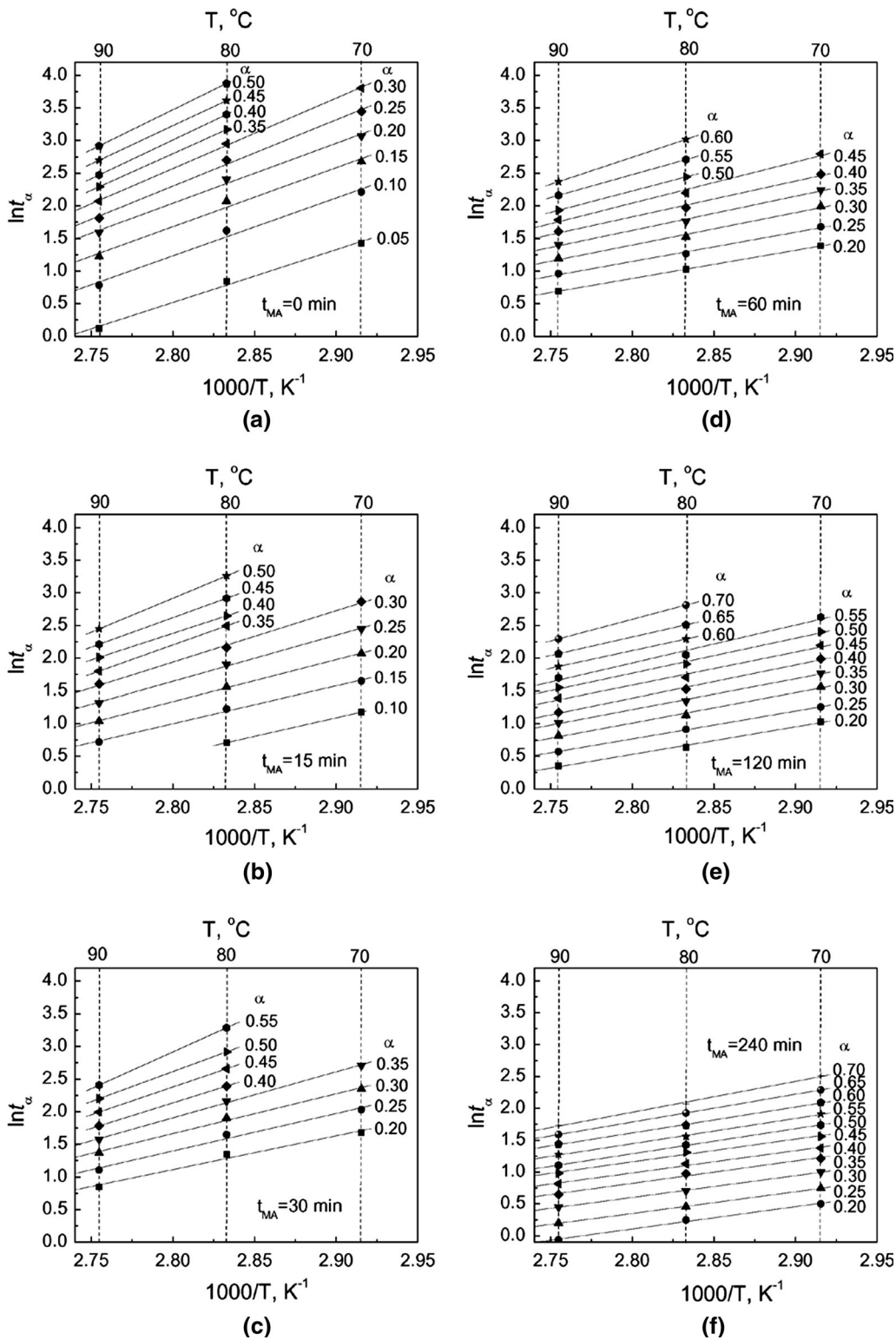
Fig. 4—$\ln t_\alpha$ vs $1/T$ plots for different values of fraction leached (α): (a) non-activated boehmite sample (t_{MA} = 0 min), (b) through (f) samples mechanically activated for different time (t_{MA} = 15, 30, 60, 120, and 240 min, respectively).

to very fine level (Figures 7(a), (b)) are leached preferentially leaving behind small clusters of very fine particles (Figure 7(c)). Higher leachability of 240 minutes milled sample *vis-à-vis* 60 minutes milled sample is evident from the micrographs of the leach residues.

Except for the increased leaching, the nature of 5, 10, and 30 minutes leached residues does not differ markedly in the case of 240 minutes milled sample (Figures 7(d) through (f)). Fine particles which appear in the leach residue of 60 minutes milled sample (Figures 7(a)

through (c)) are not readily visible in the case of 240 minutes milled sample (Figures 7(d) through (f)).

2. Particle Size distribution of leach residues

Figures 8(a) through (d) show typical particle size distribution of leach residues obtained after different
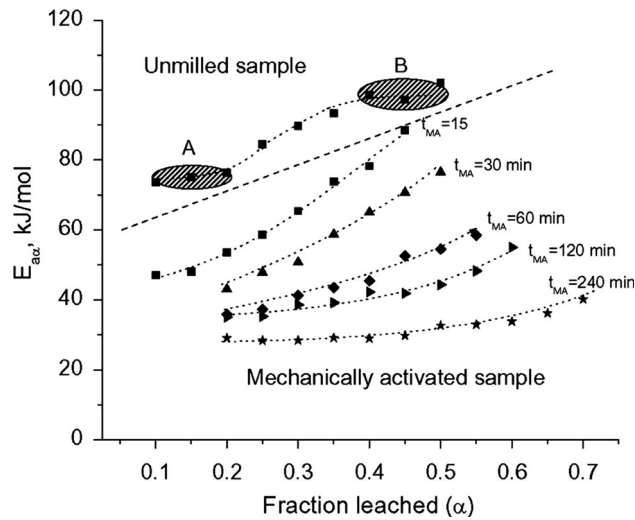

Fig. 5—Variation of apparent activation energy $E_{a\alpha}$ as a function of fraction leached for unmilled and mechanically activated boehmite samples at different activation time (t_{MA}).

duration of leaching for the samples mechanically activated for 0, 15, 60, and 240 minutes, respectively. The fraction-leached (α) values corresponding to leaching durations are also indicated in the figure. The solid lines in the figure show the particle size distribution of the residues fed into the size analyser. The actual quantities of particles are different as the amount of residue decreases with increasing leaching time. In order to take into consideration the amount of leach residue, the frequency distributions are redrawn by multiplying it with the fraction undissolved (i.e., $1-\alpha$) and shown as dotted lines. Each of the samples (t_{MA} = 0, 15, 60, and 240 minutes) shows a characteristic variation of particle size distribution with time as described below:

(i) For the non-activated sample [t_{MA} = 0 minutes, Figure 8(a)], particle size analysis shows primarily a monomodal distribution up to 20 minutes of leaching (α = 0.32). The frequency maxima of the particle size distribution occur at ~100 μm. The size distribution becomes wider with a simultaneous decrease in the frequency maxima indicating an overall decrease in the size of the particles. The nature of the particle size distribution changes from monomodal to multimodal for the leach residue obtained after 30 and 60 minutes of leaching. The multimodal character is prominent in the 60 minutes leached sample and the frequency maxima decreases rapidly from 98 μm (t = 30 minutes and α = 0.39) to 44 μm
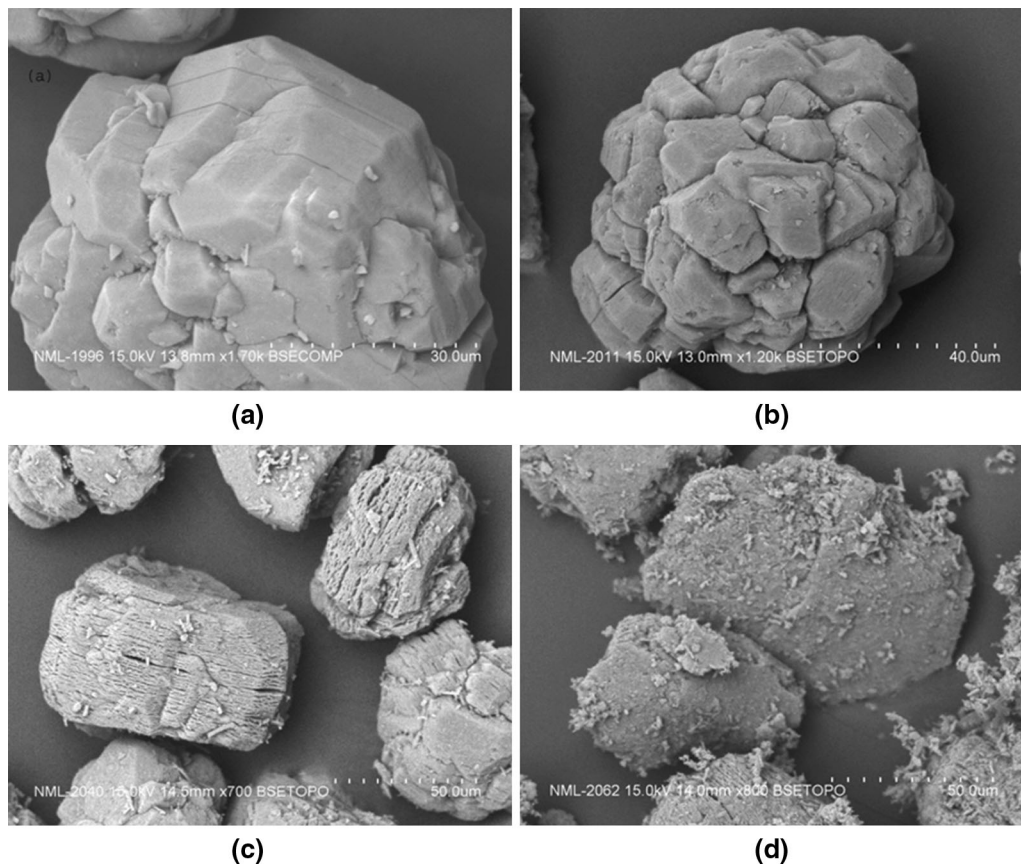

Fig. 6—SEM micrographs showing typical morphological features of leach residues obtained from non-activated boehmite after different duration of leaching : (a) 5 min; (b) 10 min; (c) 30 min; and (d) 45 min of leaching [353 K (80 °C)].
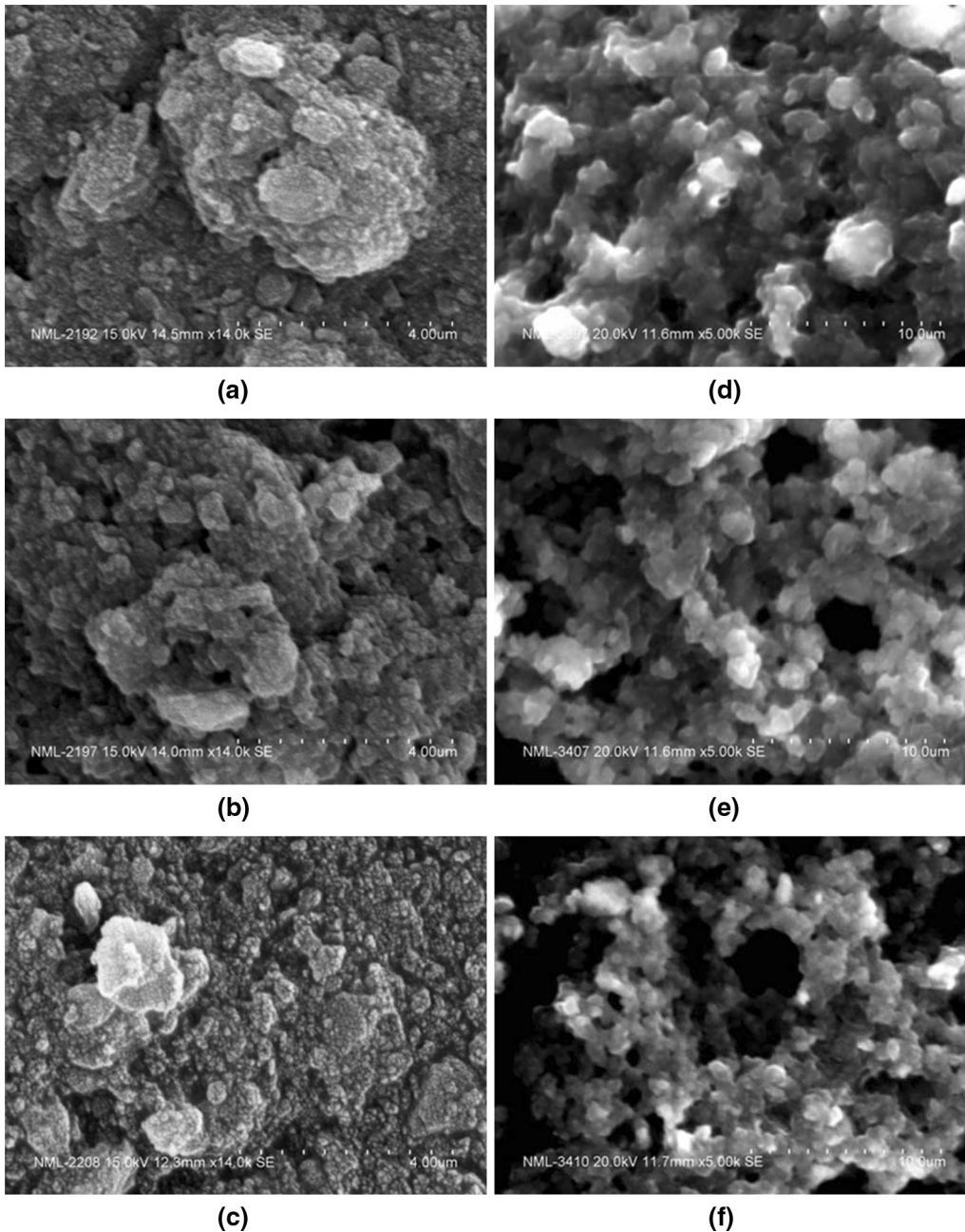
Fig. 7—SEM micrographs showing morphological features of leach residues from mechanically activated boehmite samples after different durations of leaching: (*a*), (*b*), (*c*) t_{MA} = 60 min; and (*d*), (*e*), (*f*) t_{MA} = 240 min, after 5, 20, and 30 min of leaching [353 K (80 °C)].

(t = 60 minutes and α = 0.53). These results are in agreement with the SEM observations which have indicated during initial stages of leaching preferential attacks on joints without any shape change (Figures 6(a), (b)) and fragmentation of particles at later time intervals (Figures 6(c), (d)). As reported earlier,[19] fragmentation of particles makes it difficult to apply shrinking core model to the entire range of α up to 60 minutes of leaching.

(ii) For the mechanically activated sample up to 15 minutes [t_{MA} = 15 minutes, Figure 8(b)], the multimodal size distribution character of the milled boehmite is retained up to 30 minutes of leaching

($\alpha \sim 0.5$). The lower limit of the particle size distribution span, ~0.1 μm remains unaltered while the upper limit reduces continuously from ~100 to about 53 μm after 30 minutes of leaching. This means that large size particles shrink in size or undergo fragmentation during leaching, and the rate of creation of smaller particles exceeds or is comparable to the rate of disappearance of smaller particles due to dissolution.

(iii) In the leach residue of 60 minutes activated sample [t_{MA} = 60 minutes, Figure 8(c)], initially, the particle size shows a multimodal distribution (leaching time t = 5 to 10 minutes, α = 0.35 to ~0.45).
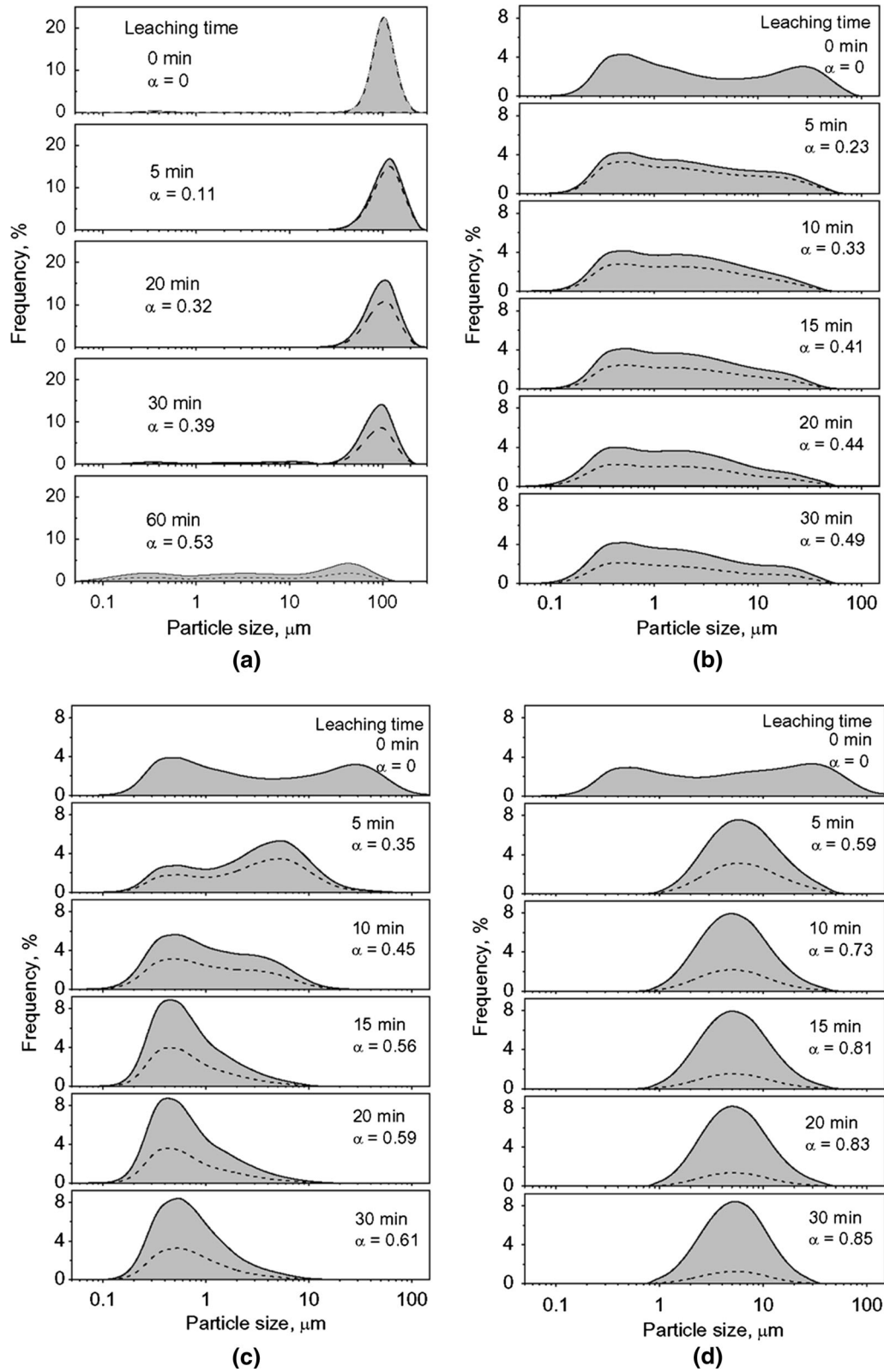
Fig. 8—Typical particle size distribution of leach residues obtained after different durations of leaching [353 K (80 °C)] for the samples mechanically activated for different times: (a) $t_{MA} = 0$ min; (b) $t_{MA} = 15$ min; (c) $t_{MA} = 60$ min; and (d) $t_{MA} = 240$ min.

However, the upper bound of the distribution rapidly diminishes and the multimodal distribution changes to a nearly monomodal one as the leaching

progresses (15 to 30 minutes, α up to ~0.6). The monomodal distribution more or less remains unchanged up to 30 minutes of leaching, since α

changes only marginally from 0.55 to 0.6 during this period. The location of the maxima in mono-modal distribution (~ 0.45 μm) nearly coincides with the lower size maxima as observed in the 5 minutes leached residue, and the height of this maxima increases with leaching time. This is possible only if the finer particles created due to leaching have comparable or lower reactivity than the fine particles created during milling. The mechanically activated particles are agglomerate of fine particles which are cemented together. SEM examination of leach residues (Figures 7(a) through (c)) appears to suggest that the cementing regions are leached faster resulting in the loosening of agglomerate structure and leaving behind finer particles which may have lower reactivity

(iv) During the leaching of 240 minutes milled sample [t_{MA} = 240 minutes, Figure 8(d)], the bimodal distribution present in the unleached disappears quite early in the 5 minutes leached sample itself (α = 0.59) and the monomodal distribution appears in the residues up to 30 minutes leaching (α = 0.85). The size distribution is characterized by a maxima at around ~5.3 μm. Interestingly, the fine particles observed at the start of leaching (t = 0 minutes) vanish very quickly within 5 minutes. This means that initially the rate of disappearance of finer particles is higher than their creation from the leaching of bigger particles. The nature of distribution stabilizes after 5 minutes which possibly indicates that there is a matching of the disappearance rate and the creation rate of the particles in a particular size range. SEM micrographs of the leach residues have also suggested that except for the increased leaching, the nature of 5, 10, and 30 minutes leached residues does not differ markedly in the case of 240 minutes milled sample and the agglomerated particles appear to behave as homogeneous entity (Figures 7(d) through (f)).

It is evident from the above observations that the state of aggregation/agglomeration of particles[22] varies uniquely with leaching time for each of the samples. Further, there are indications that the reactivity of particles formed during leaching differs from that of the milled samples before leaching. The difference in reactivity manifests with progress of leaching, depending on the milling time or the extent of mechanical activation.

3. X-ray diffraction

Select samples of the leach residues were examined by powder XRD to understand the changes in the crystalline structure during leaching. Figure 9 shows the changes in the nature of (020) XRD peak in the leach residues obtained after 5, 20, and 30 minutes from the 240 minutes mechanically activated boehmite sample. The (020) peak which is nearly flat in the unleached sample becomes less and less broad and its intensity increases continuously. This means that there is an increase in the crystallinity of leach residue with
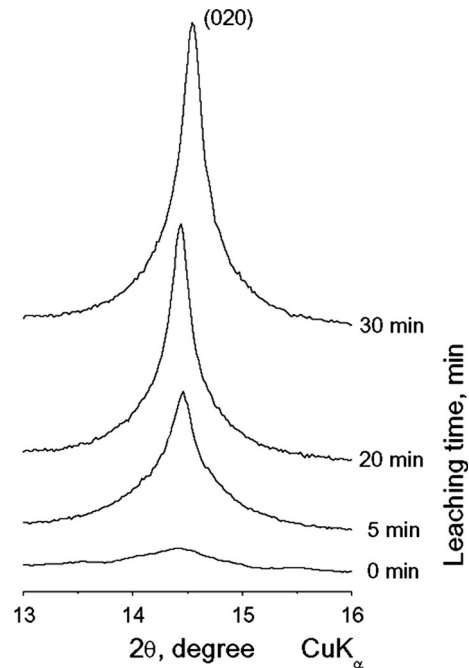

Fig. 9—XRD patterns showing change in the intensity of (002) peak for the leach residues obtained from mechanically activated boehmite (t_{MA} = 240 min) after different durations of leaching [353 K (80 °C)].

increased leaching time. In other words, the amorphous or more disordered material is preferentially leached leaving behind material which is more crystalline or ordered.

E. Reactivity of Non-activated and Mechanically Activated Boehmite

As evident from Eq. [2], the reactivity of boehmite, manifested as fraction leached (α) or rate of change of fraction leached, is closely related with activation energy. Various facets of the activation energy are discussed with respect to (a) explanation of variation in activation energy with changing characteristics of the solid phase; (b) impact of change in activation energy due to mechanical activation on rate constant; and (c) correlation between activation energy and initial physico-chemical characteristics of boehmite.

1. Apparent activation energy and structural heterogeneity

Based on the variation of apparent activation energy ($E_{a\alpha}$) with fraction leached (Figure 5), the conceptual apparent activation energy diagrams are plotted for the leaching of non-activated boehmite (t_{MA} = 0 minutes) (Figure 10(a)) and mechanically activated boehmite samples (Figures 10(b) and (c)) for t_{MA1} and t_{MA2}, such that $t_{MA2} > t_{MA1}$ (e.g., 60 and 240 minutes activated samples). The energy of the reacting solid phase is shown as a shaded band to depict variations of the energy state of the solid phase (or apparent activation energy $E_{a\alpha}$ which is a difference between energy corresponding to transition state and reacting solid) with
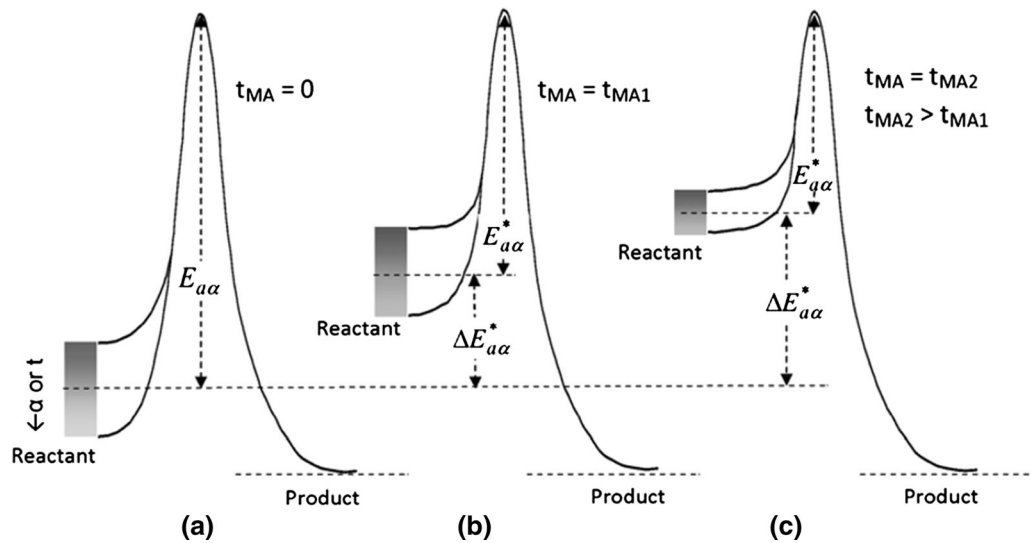
Fig. 10—The conceptual activation energy diagrams: (a) leaching of non-activated boehmite (t_{MA} = 0 min); (b), (c) mechanically activated boehmite samples for t_{MA1} and t_{MA2}, respectively ($t_{MA2} > t_{MA1}$, e.g., 60 and 120 min activated samples).

fraction leached (α) due to structural heterogeneity. The schematic diagrams in Figures 11(a) through (c), which show the changes in the nature of solid phase with fraction leached, are created based on the characterization of initial solid phase and leach residues obtained after different time intervals as described in the preceding sections. As discussed below, the observed variation $E_{a\alpha}$ with α may be explained in terms of changes in the characteristics of solid phase during leaching.

In the case of non-activated boehmite (Figures 10(a), 11(a)), the imperfections, notably joints, which are characterized by higher energy state as compared to the rest of the particle regions (e.g., crystal faces) are preferentially leached during early stages of leaching. Initially, a lower value of $E_{a\alpha}$, which is the difference between the energy corresponding to transition state and high energy regions, is observed. As the value of α increases, preferential leaching of joints and eventual breakage of particles occurs. The high energy regions diminish with an increase in α. Consequently, the gap between the energy corresponding to the transition state and the regions remaining unleached widens which manifests as an increase in the value of $E_{a\alpha}$. Based on the SEM results on leach residue, the regions marked 'A' and 'B' in Figure 5 may be ascribed to leaching dominantly from joints and crystal faces, respectively. The average value of $E_{a\alpha}$ in region A and B differs by ~23 kJ/mol. In literature,[7,9,13–17] widely different values of activation energies (73 to 120 kJ/mol) are reported for the dissolution of boehmite. Besides the method employed for kinetics analysis, the observed difference in activation energy may result due to the change in nature of solid; boehmite with greater number of grain boundaries/joints is expected to show lower value of activation energy and vice versa.

In general, mechanically activated samples are characterized by a lower value of apparent activation energy as compared to the non-activated boehmite (Figure 5). The difference in the activation energy

$$\Delta E_{a\alpha}^* = E_{a\alpha} - E_{a\alpha}^*, \qquad [6]$$

(where $E_{a\alpha}$ and E_{aa}^* are apparent activation energies for the non-activated and activated boehmite) is manifestation of stored energy which raises the energy state of the reacting solid. The stored energy increases with a decrease in microcrystallite size (MCD), increasing strain (ε), and an increase in degree of amorphization (A_m) (i.e., increase in amorphous phase).[22,23,31,34,35] It is obvious from the physico-chemical properties of mechanically activated boehmite samples (Table I), that a greater value of ΔE_{aa}^* or lowering of activation energy E_{aa}^* is expected with an increase in mechanical activation time (t_{MA}) as depicted in Figures 10(b) and (c)).

Figures 10(b) and (c) compare typical scenario for t_{MA1} (say 60 minutes) and t_{MA2} (240 minutes) samples which are characterized, respectively, by MCD, 69 and 17 nm; ε, 0.0038 and 0.0047 and degree of amorphization A_m, 61 and 86 pct. Since the sample mechanically activated for higher time (t_{MA2}) predominantly comprises amorphous phase (A_m = 86 pct), the shaded band depicting the energy of reacting phase is narrow and located higher as compared with the other sample (t_{MA1}) (A_m = 61 pct) which contains lower amounts of amorphous phase and significantly higher crystalline fraction. The amorphous phase which is characterized by higher energy is preferentially dissolved and the leach residue contains an increasing amount of crystalline phase with the progress of leaching (Figure 9). This also means an increase in apparent activation energy with fraction leached as the gap between the transition state and the energy of reacting solid widens. Based on the spread of energy for the reacting solid (Figures 10(b), (c)), a greater variability of E_{aa}^* with α is expected for sample mechanically activated for smaller time (t_{MA1}) than the sample which is mechanically activated for longer time (t_{MA2}). Variability in the nature of these samples during leaching supports this point (Figures 7 and 11(b), (c)). In case of sample mechanically activated
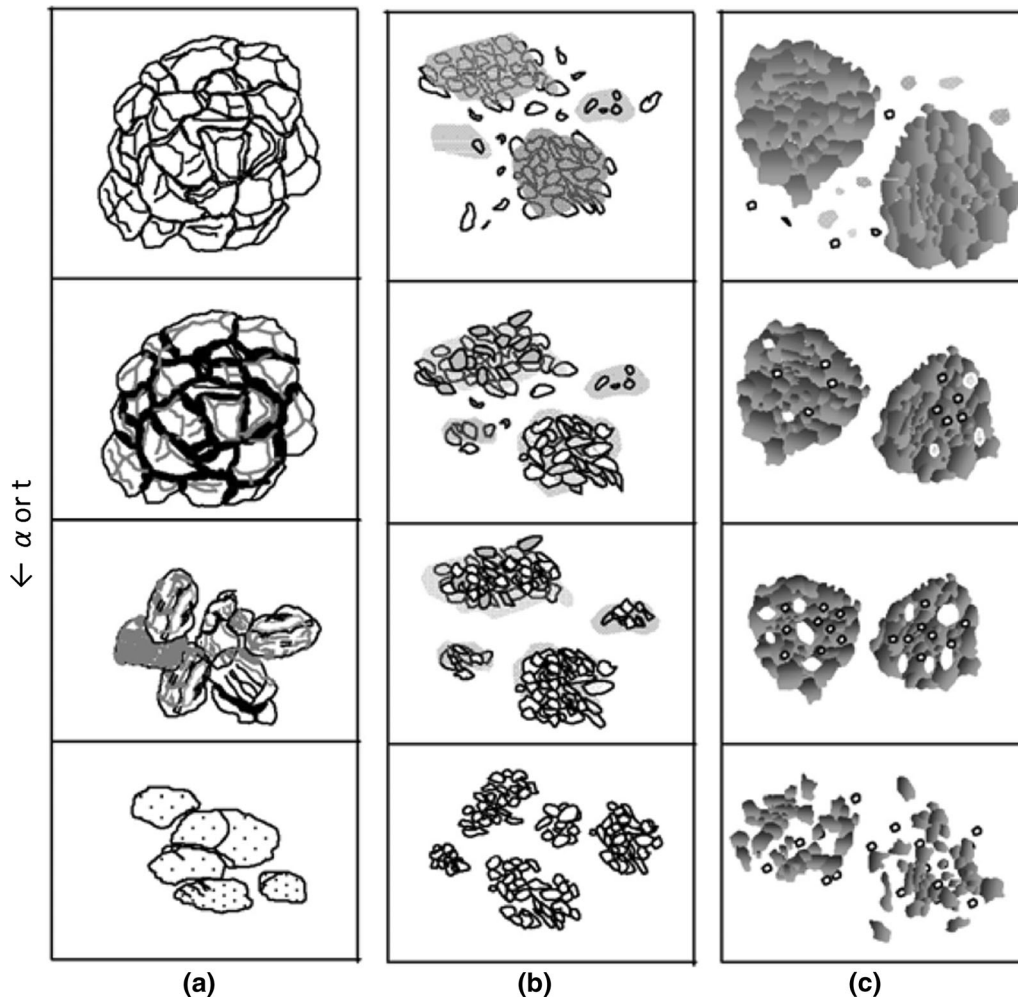
Fig. 11—The schematic diagrams showing the changes in the nature of solid phase with fraction leached: (a) non-activated boehmite—preferential dissolution at joints, leading to fragmentation followed by leaching from crystal faces; (b) mechanically activated boehmite (t_{MA1})—preferential dissolution of amorphous phase (gray) which covers the small crystallite of boehmite and also acts as a cementing phase; and (c) mechanically activated boehmite (t_{MA2})—leaching primarily dominated by the dissolution of amorphous phase [note: α scale is indicative and not same for (a), (b), and (c)].

for shorter time (*e.g.*, t_{MA1} = 60 minutes), large size crystals which are possibly cemented and coated by amorphous phase are exposed with increasing leaching time or fraction leached (Figures 7(a) through (c) and 11(b)). In case of longer milled sample (*e.g.*, t_{MA2} = 240 minutes), small size crystals having much smaller fraction remain embedded in the bulk amorphous phase and it is primarily the amorphous phase that gets leached up to an extended value of α (Figures 7(d) through (f) and 11(c)).

2. *Rate constant values in mechanically activated and non-activated boehmite*

The ratio of rate constant for the leaching of a mechanically activated and non-activated mineral is correlated with their respective apparent activation energies by Eq. [7], as follows:[23,46,47]

$$\frac{k^*}{k} = \frac{Z^*}{Z} \exp\left(\frac{\Delta E_a^*}{RT}\right), \qquad [7]$$

where k^* and k are rate constants, Z^* and Z are pre-exponential factors, and E^* and E are apparent activation energies for the activated and non-activated mineral. As indicated in Eq. [6], $\Delta E_{a\alpha}^*$ is change in apparent activation energy due to stored energy resulting from mechanical activation. In literature, a simplified form of Eq. [7] is used assuming Z^* and Z to be same. The isoconversional method does not provide the value of pre-exponential factor and it is difficult to ascertain if pre-exponential remains the same. Therefore, no assumption is made about pre-exponential factor and use of Z^* and Z is preferred. Since activation energy determined by isoconversional method (*i.e.*, $E_{a\alpha}$) varies as a function of fraction leached, it complicates the use of Eq. [7] in its proposed form. The equation can be revised to include the variability of various terms with fraction leached (α) and written as follows:

$$\left(\frac{k^*}{k}\right)_\alpha = \left(\frac{Z^*}{Z}\right)_\alpha \exp\left(\frac{\Delta E_{a\alpha}^*}{RT}\right). \qquad [8]$$
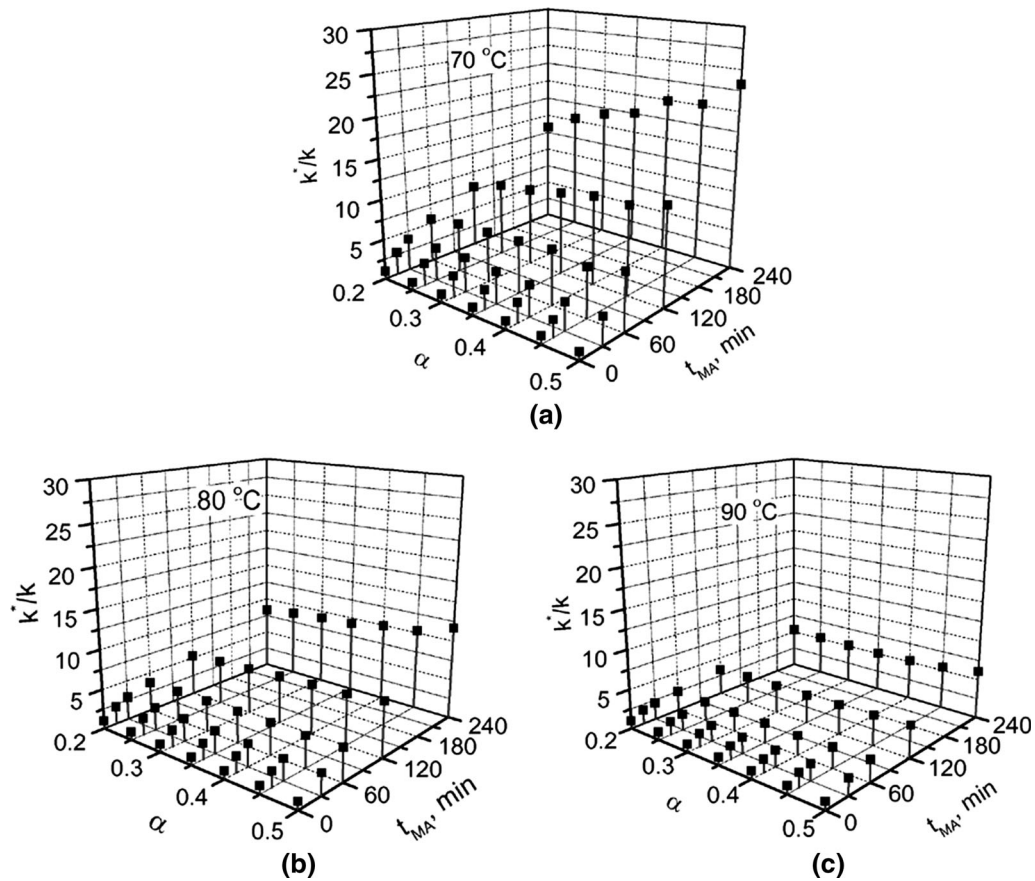
Fig. 12—Variation of rate constant ratio (k^*/k) as a function of fraction leached (α) and milling time (t_{MA}) at different leaching temperatures: (a) 343 K (70 °C); (b) 353 K (80 °C); and (c) 363 K (90 °C).

The intercepts in Figure 4 give the value of [$Z/g(\alpha)$]. Since calculation of pre-exponential factor from the intercept requires the knowledge of $g(\alpha)$, it prohibits the calculation of pre-exponential factor and rate constant. However, assuming that the form of $g(\alpha)$ remains the same for the non-activated and activated samples, the ratio of rate constant can still be calculated by modifying Eq. [8] as follows:

$$\left(\frac{k^*}{k}\right)_\alpha = \left(\frac{Z^*/g(\alpha)}{Z/g(\alpha)}\right)_\alpha \exp\left(\frac{\Delta E^*_{a\alpha}}{RT}\right). \qquad [9]$$

Figures 12(a) through (c) show the variation of (k^*/k) with fraction leached (α) and mechanical activation time (t_{MA}) at 343 K, 353 K, and 363 K (70 °C, 80 °C, and 90 °C), respectively. The dependence of (k^*/k) on α and t_{MA} is most pronounced at 343 K (70 °C) (Figure 12(a)). Irrespective of α, (k^*/k) remains more or less constant between 2 and 4 at lower milling time of 15 and 30 minutes. As the milling time increases further, (k^*/k) begins to show an increase with α and it becomes most pronounced in the 240 minutes milled sample; (k^*/k) increases from 13.3 to 23.3 with an increase in α from 0.2 to 0.5. Variation of (k^*/k) with α and t_{MA} shows similar trends at 343 K and 353 K (80 °C and 90 °C) except that the effect of milling time become increasingly less pronounced (Figures 12(b) and (c)). In the 240 minutes

milled sample, as α increases from 0.2 to 0.5, (k^*/k) increases from 8.4 to 11.7 and 5.3 to 6.1 at 343 K and 353 K (80 °C and 90 °C), respectively. The effect of temperature is as anticipated from Eq. [9].

As in earlier published studies,[23,46,47] a simplified form of Eq. [7] was also used in which pre-exponential factor (Z) is assumed to be the same for activated and non-activated mineral. The simplified Eq. [7] led to abnormally high values of (k^*/k) indicating that the assumption does not hold. When generalized Eq. [9] is used, the order of magnitude of (k^*/k) is similar to the one reported in earlier paper by Alex et al.[31] in which kinetics analysis is performed based on 'shrinking core model with surface reaction' for the non-activated boehmite and, 'first-order chemical reaction' for the mechanically activated boehmite samples. Even though the assumption regarding pre-exponential factor is relaxed, the effect of stored energy (Eq. [6]), which increases with mechanical activation time (Figures 5 and 10), on (k^*/k) is demonstrated in Figure 12. The present analysis involving isoconversional method sheds further light on α dependence of (k^*/k).

3. Correlation between activation energy and physico-chemical characteristics

The nature of correlation (r_{xy}) between activation energy $E_{a\alpha}$ (i.e., $y = E_{a\alpha = 0.2}$, $E_{a\alpha = 0.5}$) and initial
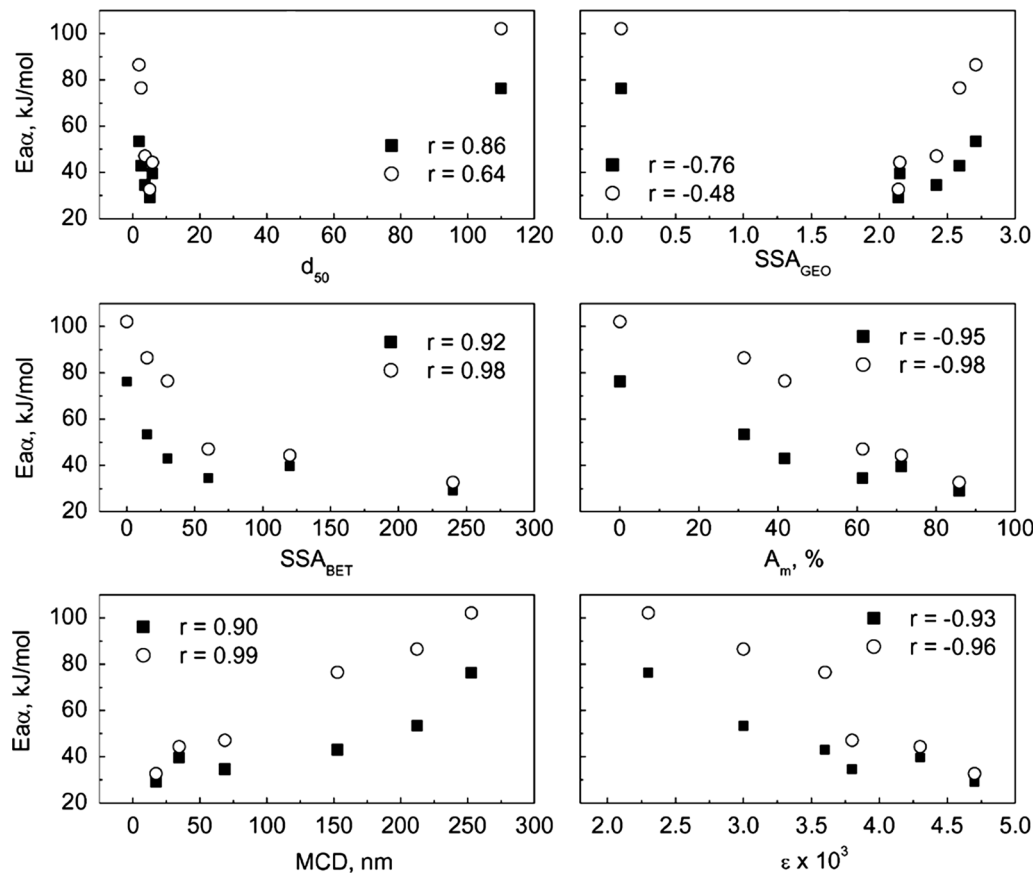
Fig. 13—The nature of correlation (r_{xy}) between activation energy $E_{a\alpha}$ ($y = E_{a\alpha\ =\ 0.2}$, $E_{a\alpha\ =\ 0.5}$) and initial sample characteristics (i.e., $x = d_{50}$, SSA_{Geo}, SSA_{BET}, A_m, MCD, and ε) (close symbols are for $E_{a\alpha\ =\ 0.2}$ and open symbols for $E_{a\alpha\ =\ 0.5}$).

sample characteristics (i.e., $x = d_{50}$, SSA_{Geo}, SSA_{BET}, A_m, MCD, and ε) was examined as shown in the scatter diagrams given in Figure 13. It is evident from the figure that the correlation coefficient between activation energy and d_{50}, SSA_{Geo} is inferior as compared to SSA_{BET}, A_m, MCD, and ε. The positive strong correlation between $E_{a\alpha}$ and SSA_{BET} is anomalous in nature and physically not significant. This is because an increase in SSA_{BET} should result in an increase in surface energy and a consequent decrease in $E_{a\alpha}$. This means that the effect of A_m, MCD, and ε on $E_{a\alpha}$ dominantly influence the leaching as compared to d_{50}, SSA_{Geo}, and SSA_{BET}. This also means that an increase in stored energy due to an increase in A_m, decrease in MCD, and increase in ε, more than offset the decrease in surface energy associated with a decrease in surface area with milling due to agglomeration of particles (Table I).[18]

F. Implications of the Results

There are a number of research papers that deal with the chemical kinetics involving reactions of mechanically activated solids.[23,48] α-t models employed to analyze the kinetics[19,23,31,38,48] are based on the assumption that the reacting solid phase is by and large homogenous in nature such that its reactivity can be described using a single rate parameter. In contrast, a model-free approach based on 'isoconversional method' is used in this

paper to analyze the kinetics of alkali leaching of non-activated and mechanically activated boehmite samples. The differences between model-fitting and model-free methods are summarized in Table II and discussed here. The structural heterogeneity, especially of mechanically activated boehmite samples, is an essential feature of all the samples. During leaching, the heterogeneity manifests itself uniquely for each of the samples. The activation energy varies as a function of fraction leached. Morphology and particle size distribution changes with the progress of leaching. In case of mechanically activated samples, crystalline nature of the samples also changes with leaching time. α-t models assume that reacting solid is structurally homogeneous and, its nature does not change with the progress of the reaction. Based on the results of this study, it can be concluded that α-t model-based analysis has limitations, except for initial rate calculation, and, there is a need to develop more rigorous models which can incorporate α dependence of activation energy and/or changing nature of reacting solid as observed in the present study. Stochastic modeling approach to chemically controlled dissolution of minerals has been in use to address the problem of differential dissolution rates resulting from structural heterogeneity.[49,50] In the developed models, a stochastic distribution for the reaction rate parameter or activation energy is assumed which may or may not be physically significant. The dependence of activation

Table II. Comparison of Model-Fitting Approach[19,31] and Model-Free Approach Used in the Present Study to Analyze the Kinetics of Alkali Leaching of Boehmite

Attribute	Approach[38]	
	Model-Fitting	Model-Free
Basic	assume a functional form for $g(\alpha)$ and kinetic model is selected based on best fit	no functional form of $g(\alpha)$ is assumed (Eq. [5])
Nature of reacting solid phase	structurally homogeneous or heterogeneity in terms of grain joints/boundaries, amorphous content, etc. do not lead to dramatically different solubility from different reacting sites	no constrain; preferred for structurally heterogeneous solids
Kinetic parameters (E_a, Z, and k)	single value for each parameter[31]	values obtained are dependent on α (Figs. 5 and 12)
Advantage/limitation	does not take into consideration the changing nature of solid during leaching provides values of all kinetic parameters	more realistic as changes in the nature of solid can be correlated with α dependence of activation energy (Figs. 5, 10, and 11); for estimation of Z (or k) requires knowledge of $g(\alpha)$; for activated solid, (k^*/k) ratio can be estimated (Eq. [9])

energy and rate constant on fraction leached, as determined by model-free kinetics analysis and supported by extensive stage-wise characterization of leach residues, is expected to impart greater significance to the development of the more rigorous and physically significant models.

IV. SUMMARY AND CONCLUSIONS

In this paper, analysis of the kinetics of leaching by 'isoconversional method' and characterization of leach residues in terms of morphology, particle size distribution, and crystallinity are used to elucidate the manifestation of the nature of structural heterogeneity during alkali leaching of non-activated and mechanically activated boehmite synthesized by thermal dehydration of boehmite. The samples were mechanically activated for 5, 15, 30, 60, 120, and 240 minutes. The leaching was carried out between 343 K and 363 K (70 °C and 90 °C) using Na_2O concentration of 180 g/l and stirring speed of 400 min^{-1}. The major conclusions are as follows:

1. The limitations of model-fitting methods used in earlier research to analyze the kinetics of dissolution of the boehmite are highlighted.
2. A sample-dependent increase in apparent activation energy with the fraction leached is observed which is correlated with the physico-chemical changes in the solid during leaching.
3. The activation energy for the leaching of non-activated boehmite varies between 75 and 98 kJ/mol. The lower value corresponds to the initial leaching regime during which leaching is dominated by preferential dissolution from crystal joints/boundaries. Increasing value of activation energy relates to the diminishing influence of dissolution from joints and the increasing influence of leaching from crystal faces.
4. The apparent activation energy for the activated samples depends on mechanical activation time. For a range of fraction leached (0.2 to 0.5), the activation energy decreases from the range 53 to 91 kJ/mol to 29 to 33 kJ/mol as the mechanical activation time increases from 15 to 240 minutes (lower values, i.e., 53 and 29 kJ/mol correspond to fraction-leached value of 0.2).
5. For the mechanically activated sample, the observed variation of apparent activation energy with fraction leached can be explained in terms of physico-chemical characteristics of the samples.

   (a) The amorphous constituent present in the samples dissolves preferentially vis-à-vis crystalline constituent.
   (b) In the 240 minutes milled sample, characterized by highest degree of amorphization (A_m = 86 pct), and least amount of crystalline material with MCD of 17 nm and strain 0.0047, least variation in apparent activation energy with fraction leached is observed. In contrast, the sample which was mechanically activated for least time (15 minutes) and characterized by lower degree of amorphization (A_m = 31.4) and higher amount of crystalline

phase (MCD = 212.2 nm and strain = 0.0030), the structural heterogeneity of the sample was manifested by a strong dependence of apparent activation energy on the fraction leached.

6. The decrease in apparent activation energy with mechanical activation results in an increase in rate constant *vis-à-vis* non-activated boehmite. The magnitude of increase is dependent on mechanical activation time, fraction leached, and leaching temperature. The highest, 23-fold increase is observed in the sample mechanically activated for the longest duration of 240 minutes and, at lower leaching temperature of 343 K (70 °C) for the fraction-leached value of 0.5.

7. An analysis of correlation between apparent activation energy and initial physico-chemical characteristics of boehmite samples indicates that the influence of degree of amorphization (A_m), MCD, and strain (ε) dominates over parameters linked with specific surface area (namely d_{50}, SSA_{Geo}, and SSA_{BET}).

NOMENCLATURE

α	Fraction leached
a, b, c	Lattice parameters (nm)
a/c	Alkali to caustic weight ratio
A_m	Degree of amorphization (pct)
d_{10}, d_{50}, d_{90}	Characteristic particle diameters (μm)
ε	Microstrain
E_a	Activation energy (kJ/mol)
$E_{a\alpha}, E_{a\alpha}^*$	α dependent E_a (kJ/mol)
$\Delta E_{a\alpha}^*$	Stored energy $E_{a\alpha} - E_{a\alpha}^*$ (kJ/mol)
$g(\alpha)$	Functional form of integrated reaction model
k/k^*	Rate constant ratio
MCD	Microcrystallite size (nm)
R	Gas constant
R^2	Correlation coefficient
r_{xy}	Binary correlation coefficient
SSA_{Geo}	Geometrical specific surface area (m^2/g)
SSA_{BET}	BET specific surface area (m^2/g)
t_{MA}	Milling or mechanical activation time (min)
t	Leaching or reaction time (min)
t_{α}	Leaching time for fraction leached α (min)
T	Temperature (K)
Z, Z^*	Pre-exponential factor

REFERENCES

1. C. Marquez-Alvarez, N. Zilkova, J. Perez-Pariente, and J. Cejka: *Catal. Rev.*, 2008, vol. 50, pp. 222–86.
2. T.C. Alex, Rakesh Kumar, S.K. Roy and S.P. Mehrotra: in *Light Metals 2012*, C.E. Suarez, ed., The Minerals, Metals & Materials Society (TMS), Warrendale, PA, 2012, pp. 15–19.
3. J.J. Kotte: in *Light Metals 1981*, P.G. Campbell, ed., The Minerals, Metals & Materials Society (TMS), Warrendale, PA, 1981, pp. 46–81.
4. R.A. Peterson, G.J. Lumetta, B.M. Rapko, and A.P. Poloski: *Sep. Sci. Technol.*, 2007, vol. 42, pp. 1719–30.
5. A.S. Russell, J.D. Edwards, and C.S. Taylor: *J. Met.*, 1955, vol. 203, pp. 1123–28.
6. R.F. Scotford and J.R. Glastonbury: *Can. J. Chem. Eng.*, 1971, vol. 49, pp. 611–16.
7. R.F. Scotford and J.R. Glastonbury: *Can. J. Chem. Eng.*, 1972, vol. 50, pp. 754–58.
8. A. Packter and H.S. Dhillon: *Z. Phys. Chem.*, 1975, vol. 256, pp. 801–807.
9. A. Packter: *Colloid Polym. Sci.*, 1976, vol. 254, pp. 1024–29.
10. T. Ejima, K. Shimakage, and K. Agatsuma: *J. Japan Inst. Light Met.*, 1980, vol. 30 (2), pp. 98–105 (in Japanese with English abstract).
11. N.S. Maltz, V.M. Sizyakov and N.S. Shmorgunenko: in *Light Metals 1983*, E.M. Adkins, ed., The Minerals, Metals & Materials Society (TMS), Warrendale, PA, 1983, pp. 99–107.
12. D. Panias, P. Asimidis, and I. Paspaliaris: *Hydrometallurgy*, 2001, vol. 59, pp. 15–29.
13. R.L. Russell and R.A. Peterson: *Ind. Eng. Chem. Res.*, 2010, vol. 49, pp. 4542–45.
14. H. Grénman, T. Salmi, D.Y. Murzin, and J. Addai-Mensah: *Hydrometallurgy*, 2010, vol. 102, pp. 22–30.
15. I. Djuric, I. Mihajlovic, Z. Zivkovic, and R. Filipović: *Chem. Eng. Commun.*, 2010, vol. 197, p. 1485.
16. I. Djuric, I. Mihajlovic, and Z. Zivkovic: *Can. Metall. Q.*, 2010, vol. 49 (3), pp. 209–18.
17. B. Li, Z. Ting-an, D. Zhi-he, L. Guo-zhi, G. Yong-nan, N. Pei-yuan, W. Xu-jian, and M. Jia: *Trans. Nonferrous Met. Soc.*, 2011, vol. 21, pp. 173–78.
18. T.C. Alex, Rakesh. Kumar, S.K. Roy, and S.P. Mehrotra: *Powder Technol.*, 2011, vol. 208, pp. 128–36.
19. T.C. Alex, Rakesh. Kumar, S.K. Roy, and S.P. Mehrotra: *Hydrometallurgy*, 2013, vol. 137, pp. 23–32.
20. W.H. Casey and B. Bunker: *Rev. Mineral. Geochem.*, 1990, vol. 23 (1), pp. 397–26.
21. A.P. Prosser: *Hydrometallurgy*, 1996, vol. 41 (2–3), pp. 119–53.
22. Z. Juhasz and L. Opoczky: *Mechanical Activation of Minerals by Grinding: Pulverizing and Morphology of Particles*, Akademiai kiado, Budapest, 1990.
23. P. Baláž, M. Achimovičová, M. Baláž, P. Billik, Z. Cherkezova-Zheleva, J.M. Criado, F. Delogu, E. Dutková, E. Gaffet, F.J. Gotor, Rakesh. Kumar, I. Mitov, T. Rojac, M. Senna, A. Streletskii, and K. Wieczorek-Ciurowa: *Chem. Soc. Rev.*, 2013, vol. 42, pp. 7571–37.
24. F. Pawlek, M.J. Kheiri, and R. Kammel: in *Light Metals 1992*, E.R. Cutshall, ed., The Minerals, Metals and Materials Society (TMS), Warrendale, PA, 1992, pp. 91–95.
25. P.G. McCormick, T. Picaro, and P.A.I. Smith: *Miner. Eng.*, 2002, vol. 15, pp. 211–14.
26. T.C. Rakesh Kumar, M.K. Alex, Z.H. Jha, S.P. Khan, S.P. Mahapatra, and C.R. Mishra : in *Light Metals 2004*, P. Crepeau, ed., The Minerals, Metals & Materials Society, Warrendale, PA, pp. 31–34.
27. T.C. Rakesh Kumar, Z.H. Alex, S.P. Khan, and S.P. Mehrotra: in *Light Metals 2005*, H. Kvande, ed., The Minerals, Metals & Materials Society, Warrendale, PA, 2005, pp. 77–79.
28. S. Fortin and G. Forté: in *Light Metals 2007*, M. Sorlie, ed., The Minerals, Metals & Materials Society, Warrendale, PA, 2007, pp. 87–92.
29. E. Taskin, K. Yidiz, and A. Alp: *Miner. Metall. Process.*, 2009, vol. 26 (4), pp. 222–25.
30. G. Greifzu: Diploma Thesis, Institute of Nonferrous Metallurgy and Purest Materials, TU Freiberg, 2012.

31. T.C. Alex, Rakesh. Kumar, S.K. Roy, and S.P. Mehrotra: *Hydrometallurgy*, 2014, vols. 144–145, pp. 99–106.
32. V.K. Smolyakov, O.V. Lapshin, and V.V. Boldyrev: *Theor. Found. Chem. Eng.*, 2008, vol. 42 (1), pp. 54–59.
33. E.V. Bogatyreva, A.G. Ermilov, and K.V. Podshibyakina: *Inorg. Mater.*, 2009, vol. 5 (12), pp. 1375–81.
34. N.J. Welham and D.J. Llewellyn: *Miner. Eng.*, 1998, vol. 11, pp. 827–41.
35. A.M. Kalinkin and E.V. Kalinkina: *Hydrometallurgy*, 2011, vol. 108, pp. 189–94.
36. S. Vyazovkin: *Thermochim. Acta*, 2000, vol. 355, pp. 155–63.
37. A. Khawam and D.R. Flanagan: *Thermochim. Acta*, 2005, vol. 429, pp. 93–102.
38. A. Khawam and D.R. Flanagan: *J. Pharm. Sci.*, 2006, vol. 95 (3), pp. 472–98.
39. A.I. Vogel: *Vogel's Textbook of Quantitative Chemical Analysis*, 5th ed. (revised by G. H. Jeffery *et al.*), Longman Group U.K. Limited, 1989.
40. M. Kitamura and M. Senna: *Adv. Powder Technol.*, 2001, vol. 12 (2), pp. 215–26.
41. D. Panias and I. Paspaliaris: *ERZMETALL*, 1999, vol. 52 (11), pp. 585–95.
42. W. Chesworth: *Clay Clay Miner.*, 1972, vol. 20, pp. 369–74.
43. K. Wefers: *Metall*, 1967, vol. 25 (5), pp. 422–31.
44. K. Wefers and C. Misra: *Oxides and Hydroxides of Aluminum*, Alcoa Technical Paper No. 19, Revised, Alcoa Laboratories, 1987.
45. J.A. Apps, J.M. Neil, and C. Jun: "Thermochemical Properties of Gibbsite, Bayerite, Boehmite, Diaspore and the Aluminate ion Between 273 K and 623 K (0 °C and 350 °C)", Report No. LBL-21482, US Department of Energy, August 1988.
46. P. Baláž: *Extractive Metallurgy of Activated Minerals*, Elsevier, Amsterdam, 2000.
47. A.N. Zelikman, G.M. Voldman, and L.V. Beljajevskaja: *Theory of Hydrometallurgical Processes*, Metallurgija, Moscow, 1975 (in Russian) (cited in Reference 46).
48. P. Baláž: *Mechanochemistry in Nanoscience and Minerals Engineering*, Springer, Heidelberg, 2008.
49. J.J.C. Jansz: *Hydrometallurgy*, 1984, vol. 12 (2), pp. 225–43.
50. A. Lüttge, R.S. Arvidson, and C. Fis: *Elements*, 2013, vol. 9 (3), pp. 183–88.